Ion explosion and multi-mega-electron-volt ion generation from an underdense plasma layer irradiated by a relativistically intense short-pulse laser

M. Yamagiwa, J. Koga, L. N. Tsintsadze, Y. Ueshima, and Y. Kishimoto*
Advanced Photon Research Center, Japan Atomic Energy Research Institute, 1-1-2, Umemidai 8-chome, Kizu-cho, Soraku-gun, Kyoto 619-0215, Japan
(Received 16 March 1999)

Ion acceleration and expansion in the interaction of a relativistically intense short-pulse laser with an underdense plasma layer are investigated. Ion and electron dynamics are studied by a two-dimensional particle-in-cell simulation with the real mass ratio. It is shown that the longitudinal electric field induced by electron evacuation due to a large ponderomotive force or light pressure can accelerate ions to several MeV in the direction of the laser propagation. It is after the laser completely passes through the plasma layer that the ion explosion starts to be significant. [S1063-651X(99)04611-5]

PACS number(s): 52.40.Nk, 52.65.Rr

I. INTRODUCTION

Fast ion production [1–3] as well as fast electron production [4] is one of the interesting new features in intense laser-matter interactions. Fast proton emission showing a sharp cutoff at a few MeV from picosecond laser interactions with solid targets was measured for the intensity range of the order of $I\sim 10^{18}\,\mathrm{W/cm^2}$ [1]. It was found that 10% of the laser energy was transferred into MeV ions. The maximum ion energy cutoff $E_{\max}$, roughly proportional to the intensity, was observed to reach 5.5 MeV. At $I\sim 10^{19}\,\mathrm{W/cm^2}$ $E_{\max}$ can reach 12 MeV. A scaling of $E_{\max}\sim I^{1/3}$ has been obtained experimentally [2]. The energetic ion emission and the sharp cutoff in the ion energy spectrum may possibly come from fast electron driven plasma expansion [5–7] and charge separation [8,9], respectively.

The high energy particles generated in intense laser-plasma interactions could be applied to high energy nuclear science such as the experimentally observed neutron production from d-d fusion reactions due to laser irradiation on a deuterated target with a peak intensity of the order of $10^{18}\,\mathrm{W/cm^2}$ [10] and $10^{19}\,\mathrm{W/cm^2}$ [11,12]. The presence of a preformed underdense plasma seemed to be crucial to the production of neutrons for the experiment [10]. Three-dimensional (3D) particle-in-cell (PIC) simulation results in Ref. [10] indicate that the occurrence of neutrons in the experiment came from the acceleration of deuterons to a few hundreds of keV in an exploding hot plasma channel. The analysis was, however, for the specific experiment, and the detailed dependence of fast ion production on preplasma and laser conditions was not clarified.

It has also been mentioned in Ref. [13] that energies of ions accelerated in the transverse direction reach 3 MeV in the interaction of an underdense plasma with a laser pulse with a peak intensity of the order of $10^{20}\,\mathrm{W/cm^2}$. MeV protons have also been found in a 2D PIC simulation of laser hole boring into an overdense plasma [14], with a hot component in the ion spectrum prescribed by a temperature $T_{ih}=0.5\,\mathrm{MeV}$ and a maximum ion energy exceeding 5 MeV for $I\sim 10^{20}\,\mathrm{W/cm^2}$. In such an overdense plasma, the laser radiation pressure compresses both electrons and ions significantly and a shock wave may be somehow concerned with the laser-plasma interaction and hence a multidimensional treatment should be indispensable in terms of the degrees of freedom of the shock wave [15]. However, only model problems can be treated multidimensionally from the viewpoint of resolving the plasma skin depth and the period of plasma oscillations for overdense plasmas [14].

A mechanism of ion acceleration in an underdense plasma may also be the aforementioned charge separation due to fast electron production. In an intense laser-plasma interaction, however, the high-frequency ponderomotive force is larger than the plasma pressure, the total pressure force changes sign, and electrons are accelerated in the direction of the laser propagation. Furthermore, the ion acceleration process is considered to depend on to what extent the electron density profile is modulated and charge balance is broken; how large the induced electrostatic field is in the course of compensation of the charge imbalance; and how long it lasts. In this paper, we study the interaction of an ultraintense short-pulse laser with an underdense plasma layer in terms of ion explosion with the electrostatic field induced by electron evacuation due to a large pondermotive force. Emphasis is placed on ion acceleration and expansion, which become more significant after the laser pulse and hence the accelerated electron front completely passes through the plasma layer. The ion acceleration and expansion are regarded as a sort of directed Coulomb explosion.

II. PIC SIMULATION

To study the problem we use a 2D fully relativistic PIC code which self-consistently solves Maxwell's equations along with the both particle motion of electrons and ions. The details of the numerical algorithm can be found in Ref. [16]. We use a system size of $120\lambda_0$ in the x (laser) direction and $60\lambda_0$ in the y (transverse) direction, where λ_0 is the incident laser wave length. We assume initially Gaussian pulses with a full width at half maximum of $4\lambda_0$ ($8\lambda_0$) in the x (y) direction. The linearly polarized laser pulse is normally incident to the preplasma layer. The laser intensity is

*Also at Naka Fusion Research Establishment, Japan Atomic Energy Research Institute, Ibaraki, Japan.

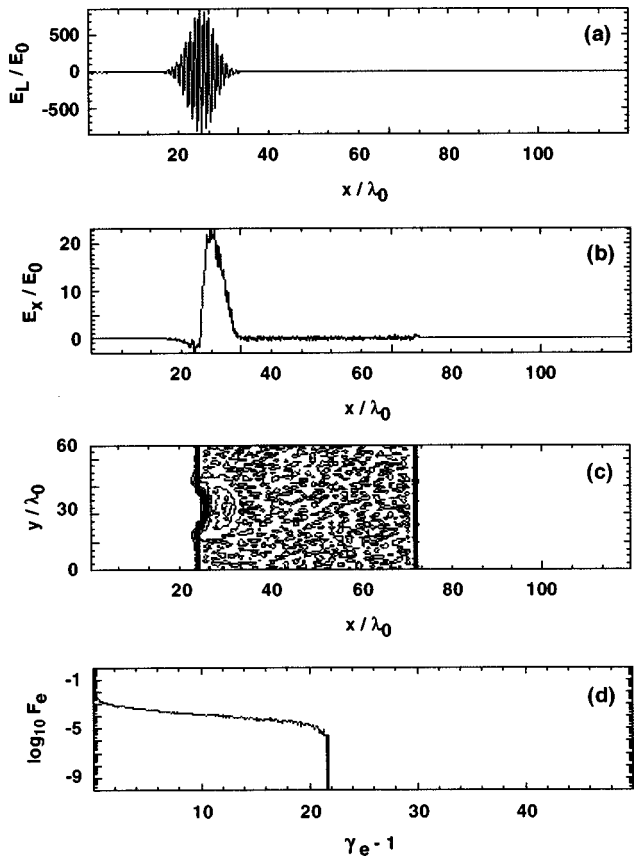

FIG. 1. Profiles of (a) the laser electric field which is propagating to the right and (b) the electrostatic field induced in the x direction at $y=30\lambda_0$, (c) the electron density contour, and (d) the electron energy spectrum for $\omega_{p0}t=20$. The parameters are $n_e=n_0$ and $I=I_0$, and the plasma layer width is taken to be $d=48\lambda_0$.

taken to be $I=I_0=10^{21}\,\mathrm{W/cm^2}$. There exists a vacuum region on both sides of the plasma layer. The length of the left vacuum region in the x direction is fixed to be $24\lambda_0$, whereas the right one (typically $48\lambda_0$) is varied depending on the plasma layer width. Depending on the length of the plasma layer, there are 2.5 to 5 particles per cell for the electrons with the same number for ions in the plasma layer. The initial temperatures are $T_e=T_i=10\,\mathrm{keV}$. The plasma density is $n_e=n_0=10^{20}\,\mathrm{cm^{-3}}$, which is less than 10% of the critical density n_c. A real proton to electron mass ratio of $m_i/m_e=1836$ is adopted.

First we show in Fig. 1 profiles of (a) the laser electric field which is propagating to the right and (b) the electrostatic field induced at the plasma boundary in the x direction at $y=30\lambda_0$, (c) the electron density contour, and (d) the electron energy distribution function for $\omega_{p0}t=20$, where ω_{p0} is the electron plasma frequency for $n_e=n_0$. The electric field is normalized by E_0 which is $4\pi n_0 e\Delta$, where e is the elementary charge and Δ is the grid size. The energy distribution function is normalized so that its integration over energy is unity. The parameters are $n_e=n_0$ and $I=I_0$, and the plasma layer width is taken to be $d=48\lambda_0$. We can see that the electrons are pushed in the propagation direction of the laser. This is because a strong high-frequency field, as considered in this paper, has the character of a compression wave [17] and the electrons acquire a velocity directed in the laser propagation direction at the leading edge. This effect

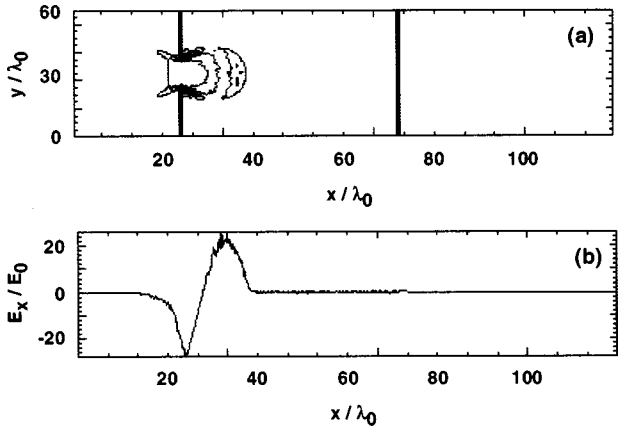

FIG. 2. (a) The electron density contour and (b) the electrostatic field in the x direction at $y=30\lambda_0$ for $\omega_{p0}t=30$.

also manifests itself in the ''sweeping up'' of electrons by the high-frequency radiation pressure. As was shown in Ref. [17], this plowing of particles is possible only in the supersonic regime if there is a relativistic nonlinearity. More precisely, this condition is analogous to the requirement that $r_0 > v_g\tau_0$ in the weak relativistic case, as was shown in Ref. [18], where r_0 is the transverse width of the laser pulse, v_g the laser propagation velocity, and τ_0 is the laser pulse length. In the strongly relativistic case, which is considered in the present work, the above condition is cast in the form $r_0 \sim v_g\tau_0$ or in terms of the ponderomotive force $\nabla\gamma$, where γ is the relativistic factor, $\nabla_\parallel\gamma > \nabla_\perp\gamma$. This condition is well satisfied for the present case.

The electron density rises at the front of the laser pulse, whereas in the region of the trailing edge of the laser pulse the electrons are braked by the ponderomotive force and the plasma behind the wave is unperturbed. The ions remain almost still, therefore an electrostatic field mainly in the laser propagation direction is induced owing to charge separation. The electron energy soon reaches up to $\sim$10 MeV corresponding to a relativistic factor of $(\gamma_e-1)\sim 20$, whereas a substantial fast ion tail does not appear.

At $\omega_{p0}t=30$ (Fig. 2), we can see (a) a shift in the peak position of the electron density, indicating somewhat of a sign of laser hole boring, and also continued pushing of electrons by the laser ponderomotive force. We can also observe electrons ejected from the boundary. This may come from the fact that the charged surface of the plasma, which borders with the vacuum, is unstable to small surface perturbations [19]. The instability is manifested in the modulation of the surface charge density. The development of this instability leads to a turbulent state, which then leads to the acceleration of particles. A negative dip is also formed in (b) the electrostatic field. At $\omega_{p0}t=40$ (Fig. 3), a local condensation or evacuation of electrons leads to a dip or cavity formation in (a) the electron density. Figure 3(b) shows that the electron energy becomes more than 20 MeV. We can also see an ion tail, reaching $\sim$0.4 MeV, in Fig. 3(c). At $\omega_{p0}t=70$ (Fig. 4), peaks both in (a) the electron density and (b) the electrostatic field continue to proceed together with the laser propagation. The electrostatic field has a wave form similar to that of a nonlinear wake.

When the laser has crossed the entire plasma layer at

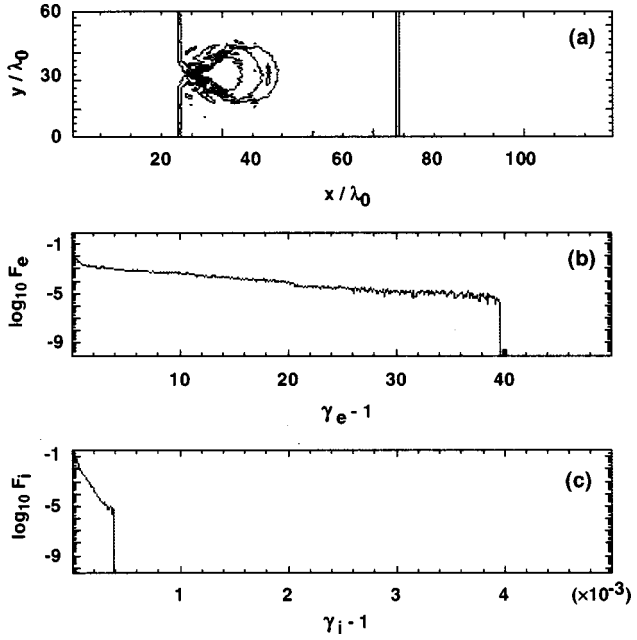

FIG. 3. (a) The electron density contour, (b) the electron energy spectrum, and (c) the ion energy spectrum for $\omega_{p0}t=40$.

$\omega_{p0}t=90$ (Fig. 5), electrons go across the original right boundary, as shown in (a). That is, some of electrons have been completely swept up from the main plasma region and subsequent separation of these electrons from the plasma layer gives rise to ion acceleration and expansion due to the charge separation. A single large peak in (b) the electrostatic field appears again near the right boundary. Figure 5(c) shows that the maximum ion energy $E_{\max}$ reaches $\sim$1 MeV. The ion maximum energy further increases up to $\sim$2 and $\sim$3 MeV, respectively, at $\omega_{p0}t=110$ and 120.

At $\omega_{p0}t=150$ (Fig. 6), electrons have moved further forward, as shown in (a). Ion acceleration and expansion near the original plasma boundary are also clearly seen, as shown in (b) the ion energy spectrum ($E_{\max}<\sim 5$ MeV) and (c) the ion density contour, respectively. Figure 6(d) shows a contour of the ion distribution in the x-P_x plane, where P_x is the ion momentum in the x direction, indicating that ions are accelerated in the x direction near the original plasma boundary.

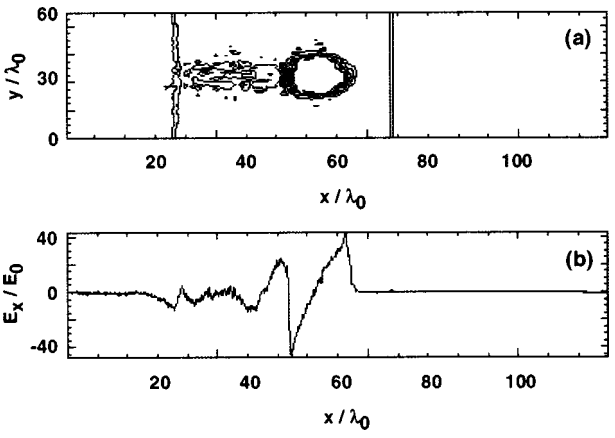

FIG. 4. (a) The electron density contour and (b) the electrostatic field in the x direction at $y=30\lambda_0$ for $\omega_{p0}t=70$.

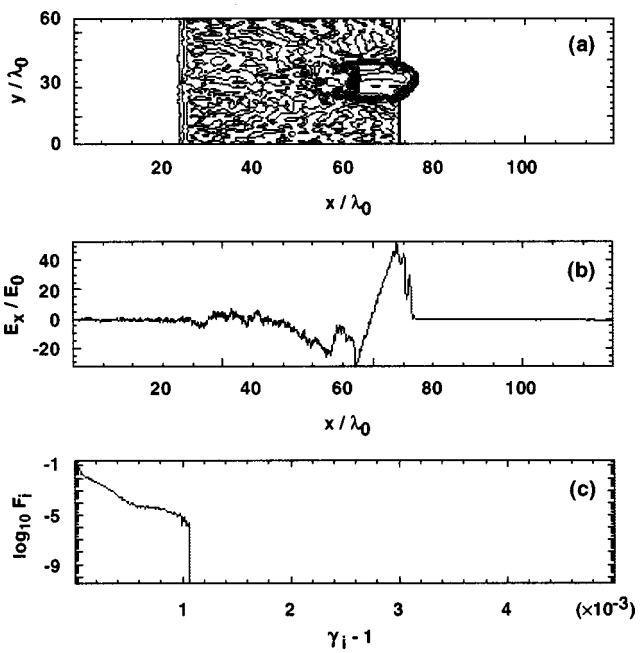

FIG. 5. (a) The electron density contour, (b) the electrostatic field in the x direction at $y=30\lambda_0$, and (c) the ion energy spectrum for $\omega_{p0}t=90$.

In this way, $E_{\max}$ rises up over a short time scale especially after the laser pulse passes through the plasma layer, as is also shown in Fig. 7, depicting the time evolution of the maximum ion energy expressed by using the relativistic factor ($\gamma_i^{\max}-1$) for $d=48\lambda_0(24\lambda_0)$. The rate of the growth of $E_{\max}$ increases after $\omega_{p0}t=100(70)$, around when the front electrons start to go through the original right boundary. It is seen that ion acceleration begins to become significant after the laser passes through the main plasma layer. Therefore, $E_{\max}$ rises up earlier in the case of shorter d. However, the value of $E_{\max}$ attained later, at $\omega_{p0}t=150$, is lower than the case of longer d. This is because more electrons can be swept out of the main plasma layer and thereby the charge separation effect is more significant for longer d. Thus, separation of electrons from the plasma layer is essential for ion acceleration and expansion and this process can also be regarded as Coulomb explosion, since it occurs on a shorter time scale.

We have also found that $E_{\max}$ roughly scales with $I^{0.5}$ and increases linearly with the plasma layer width d. This may come from the fact that the relativistic ponderomotive force, which acts on electrons, is proportional to $I^{0.5}$ and that the number of accelerated electrons which are swept up from the main plasma layer and hence the induced electrostatic field can increase linearly with d. Whether this linear increase in $E_{\max}$ with d continues is not clear. The extent to which $E_{\max}$ saturates with respect to d will be left to future study using a longer simulation.

III. CONCLUDING REMARKS

In conclusion, two-dimensional PIC simulations of the interaction of a relativistically intense short-pulse laser with an underdense plasma layer has been performed to investigate high energy proton tail formation. It has been found that a

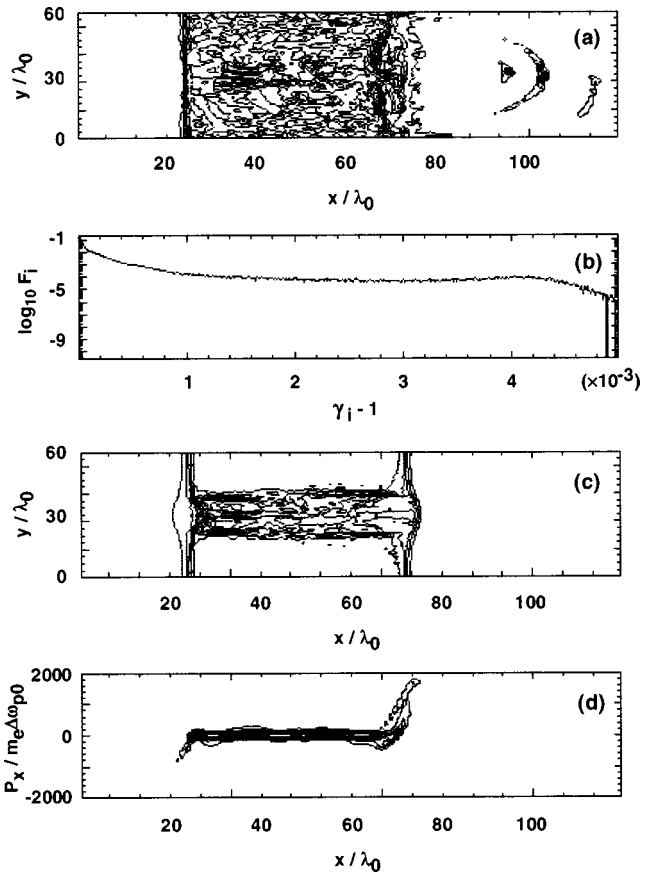

FIG. 6. (a) The electron density contour, (b) the ion energy spectrum, (c) the ion density contour, and (d) the contour of the ion distribution in the x-P_x plane for $\omega_{p0}t=150$.

large longitudinal electric field is generated by ponderomotive evacuation of electrons and that strong ion acceleration and ion expansion can take place. This process persists and becomes significant after the laser front has gone through the plasma layer, since ions follow electrons separated from the plasma layer. It has also been found that the ion tail energy can reach around 5 MeV and possibly higher for higher density.

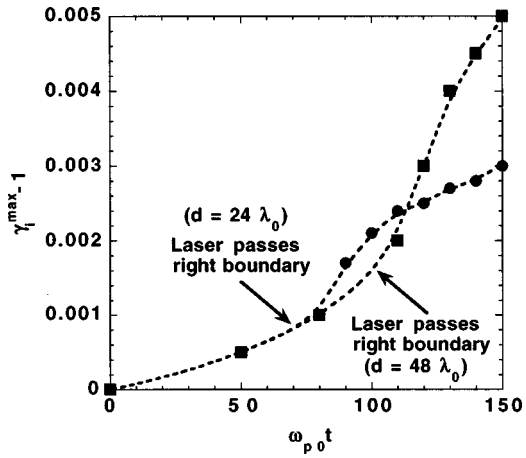

FIG. 7. The time evolution of the maximum ion energy for $d=48\lambda_0$ and $24\lambda_0$.

In Ref. [20], fast ion production by the so-called Coulomb explosion was examined in terms of laser-cluster interaction. In this scheme, light ions like protons and deuterons as well as highly charged ions may be energetic at moderate laser power. However, the ions are accelerated in all directions. In the scheme presented in this paper, unidirectional multi-MeV ion generation from relativistically intense laser-plasma interactions is a possibility. Application of fast ions produced in the interaction of an ultrahigh intense laser with plasmas to nuclear science such as nuclear transformation due to (p,n) reactions will be presented elsewhere in the near future.

The effects of collisions, which may suppress the high energy ion tail formation, should be examined. Higher density (critical to overdense) and more thick plasma layer cases and longer time scale behavior with larger system size are also left for future studies.

ACKNOWLEDGMENTS

We would like to thank Mr. K. Nakagawa for maintenance of the PIC code. It is also a pleasure to acknowledge valuable conversations with Dr. T. Tajima and Dr. T. Arisawa.

[1] A. P. Fews *et al.*, Phys. Rev. Lett. **26**, 1801 (1994).
[2] F. N. Beg *et al.*, Phys. Plasmas **4**, 447 (1997).
[3] B. Rau and T. Tajima, Phys. Plasmas **5**, 3575 (1998).
[4] G. Malka *et al.*, Phys. Rev. Lett. **79**, 2053 (1997).
[5] L. Wickens, J. E. Allen, and P. T. Rumsby, Phys. Rev. Lett. **41**, 243 (1978).
[6] M. A. True, J. R. Albritton, and E. A. Williams, Phys. Fluids **24**, 1885 (1981).
[7] A. V. Gurevich and A. P. Meshcherkin, Zh. Eksp. Teor. Fiz [Sov. Phys. JETP **53**, 937 (1981)].
[8] J. S. Pearlman and R. L. Morse, Phys. Rev. Lett. **40**, 1652 (1978).
[9] Y. Kishimoto, K. Mima, T. Watanabe, and K. Nishikawa, Phys. Fluids **26**, 2308 (1983).
[10] G. Pretzler *et al.*, Phys. Rev. E **58**, 1165 (1998).
[11] P. A. Norreys *et al.*, Plasma Phys. Controlled Fusion **40**, 175 (1998).
[12] L. Disdier, J-P. Garconnet, G. Malka, and J-L. Miquel, Phys. Rev. Lett. **82**, 1454 (1999).
[13] A. Pukhov and J. Meyer-ter-Vehn, Phys. Rev. Lett. **76**, 3975 (1996).
[14] A. Pukhov and J. Meyer-ter-Vehn, Phys. Rev. Lett. **79**, 2686 (1997).
[15] S. C. Wilks and W. L. Kruer, IEEE J. Quantum Electron. **33**, 1954 (1997).
[16] C. K. Birdsall and A. B. Langdon, in *Plasma Physics via Computer Simulation* (McGraw-Hill, New York, 1985).
[17] N. L. Tsintsadze and D. D. Tskhakaya, Zh. Eksp. Teor. Fiz. [Sov. Phys. JETP **45**, 252 (1977)].
[18] L. N. Tsintsadze, K. Mima, and K. Nishikawa, in *Superstrong Fields in Plasmas*, edited by M. Lontano, AIP Conf. Proc. No. 426 (AIP, Woodbury, NY), p. 176.
[19] L. N. Tsintsadze, Phys. Plasmas **5**, 4107 (1998).
[20] T. Ditmire, Phys. Rev. A **57**, R4094 (1998).